

RSC Advances

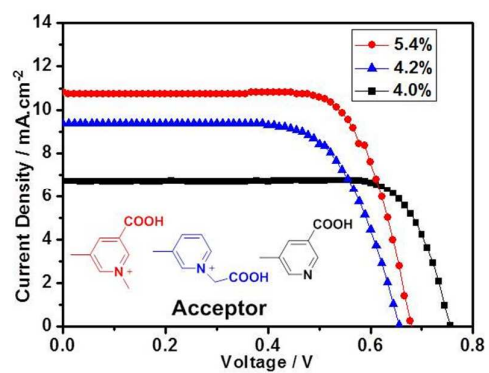


This is an *Accepted Manuscript*, which has been through the Royal Society of Chemistry peer review process and has been accepted for publication.

Accepted Manuscripts are published online shortly after acceptance, before technical editing, formatting and proof reading. Using this free service, authors can make their results available to the community, in citable form, before we publish the edited article. This *Accepted Manuscript* will be replaced by the edited, formatted and paginated article as soon as this is available.

You can find more information about *Accepted Manuscripts* in the [Information for Authors](#).

Please note that technical editing may introduce minor changes to the text and/or graphics, which may alter content. The journal's standard [Terms & Conditions](#) and the [Ethical guidelines](#) still apply. In no event shall the Royal Society of Chemistry be held responsible for any errors or omissions in this *Accepted Manuscript* or any consequences arising from the use of any information it contains.



A systematical investigation of the organic D- π -A sensitizers with different pyridiniums as acceptor group when compared to the reference dye

Cite this: DOI: 10.1039/c0xx00000x

www.rsc.org/xxxxxx

ARTICLE TYPE

Organic D- π -A sensitizer with pyridinium as acceptor group for dye-sensitized solar cells

Jie Tian,^a Xichuan Yang,^{*a} Jianghua Zhao,^a Lei Wang,^a Weihan Wang,^a Jiajia Li^a and Licheng Sun^{a,b}

Received (in XXX, XXX) Xth XXXXXXXXXX 20XX, Accepted Xth XXXXXXXXXX 20XX

DOI: 10.1039/b000000x

Two metal-free organic dyes with triphenylamide (TPA) as donor group and pyridinium (m-carboxyl-*N*-methylpyridinium and *N*-methylcarboxylpyridinium) as acceptor and anchoring group have been synthesized for dye-sensitized solar cells (DSSCs). A systematical investigation of the relationship between the structures and physical, electrochemical and photovoltaic properties has been conducted. The devices sensitized by **TJ101** which employed m-carboxyl-*N*-methylpyridinium as acceptor group has achieved the conversion efficiency of 5.4% ($J_{sc} = 10.8 \text{ mA cm}^{-2}$, $V_{oc} = 680 \text{ mV}$, $FF = 74.2\%$) under AM 1.5 irradiation. In contrast, much lower efficiency of 4.0% was obtained when a reference dye **TJ101R** with m-carboxylpyridine as acceptor group was employed as sensitizer.

Introduction

Dye-sensitized solar cells (DSSCs) have attracted significant attention due to its low cost and high power conversion since Grätzel and coworkers firstly reported it with an impressive efficiency of 7.9%.¹ So far, a record power conversion efficiency of 13% has been achieved.² As a key component, a variety of efficient sensitizers have been designed to get higher power conversion efficiency for DSSCs, such as ruthenium polypyridyl complexes,³⁻⁵ porphyrin sensitizers⁶⁻¹³ and metal-free organic dyes.¹⁴⁻²² Concerning the cost and limited ruthenium resource and the low yield of porphyrin sensitizers, metal-free organic dyes have received much attention due to high molar extinction coefficient, ease of tunable molecular structure and low cost. In these dyes, cyano acrylic acid are usually served as acceptor and anchoring group.^{14, 19-22} However, compared with electron donor groups, there are few reports on the investigation of electron acceptor groups. Recently, pyridine derivatives as acceptor groups have been successfully applied in DSSCs for the strong electron withdrawing ability and excellent charge injection ability.²³⁻²⁶ Hydroxypyridium served as electron acceptor and anchoring group in DSSCs was reported by our group.²³ It is reasonable to replace the hydroxyl group with the carboxyl group to strengthen the withdrawing ability of acceptor group and anchoring group for higher photon-to-electron conversion efficiency.

In this paper, two pyridinium dyes (**TJ101** and **TJ102**) with alkoxy triphenylamide as donor group, vinylthiophenyl as π -bridge group and pyridinium (m-carboxyl-*N*-methylpyridine and *N*-methylcarboxylpyridine) as acceptor group have been

synthesized to study the effect of the pyridinium unit and the position of carboxyl on the performance of DSSCs. The structures of the sensitizers (**TJ101-TJ102** and **TJ101R**) are shown in Figure 1 and the specific synthetic steps are displayed in the supporting information.

Results and discussion

Photophysical and electrochemical properties

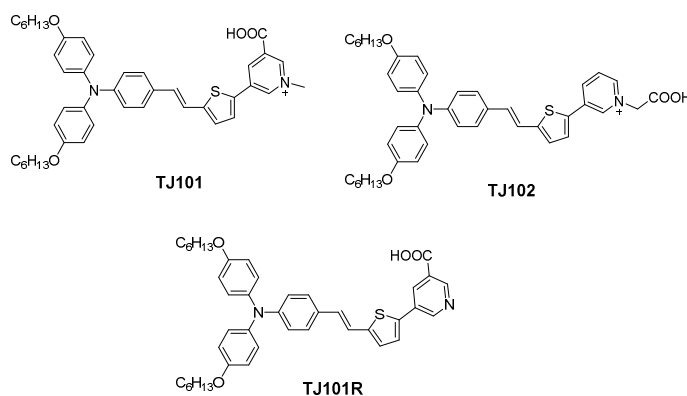


Fig.1 Structures of **TJ101**, **TJ102** and **TJ101R**

The UV-Visible absorption spectra of **TJ101**, **TJ102** and **TJ101R** in a diluted solution of CH_2Cl_2 and on TiO_2 film are shown in Figure 2. The corresponding data are collected in Table 1. All the dyes have two absorption maxima: the absorption band at 300-350 nm is ascribed to $S_0 \rightarrow S_2$ transition and the band at

around 430-470 nm can be assigned to $S_0 \rightarrow S_1$ transition. The maximal absorption for **TJ101R**, **TJ101** and **TJ102** are located at 424 nm ($\epsilon = 34600 \text{ mol}^{-1} \text{ cm}^{-1}$), 459 nm ($\epsilon = 31000 \text{ mol}^{-1} \text{ cm}^{-1}$), 455 nm ($\epsilon = 25900 \text{ mol}^{-1} \text{ cm}^{-1}$), respectively. In contrast to **TJ101R**, the maximal absorption peak of **TJ101** and **TJ102** are red-shifted 35 nm and 31 nm, respectively, indicating that the introduction of pyridinium can increase the electron withdrawing

ability of the electron acceptor. In addition, compared to **TJ102**, **TJ101** exhibits a little red-shifted maximal absorption peak and high molar extinction coefficient, which is probably due to a better withdrawing synergistic effect of carboxyl group with pyridinium ring for **TJ101** than that for **TJ102**.

The absorption spectra of the **TJ** series of dyes adsorbed on the TiO_2 film are shown in Figure 2b. Obviously, the absorption

Table 1 Absorption and electrochemical data of the sensitizers **TJ101**, **TJ102** and **TJ101R**

Dye	λ_{max}^a (nm)	ϵ at λ_{max} ($\text{M}^{-1} \cdot \text{cm}^{-1}$)	λ_{max}^b on film (nm)	E_{0-0}^c (eV)	E_{HOMO}^d (V) (vs. NHE)	E_{LUMO}^e (V) (vs. NHE)
TJ101	459	31000	449	2.23	0.61	-1.62
TJ102	455	25900	444	2.30	0.62	-1.68
TJ101R	424	34600	401	2.54	0.67	-1.87

^a Absorption spectra were measured in CH_2Cl_2 solution ($2 \times 10^{-5} \text{ M}$). ^b Absorption spectra on TiO_2 film were measured with dye-loaded TiO_2 film immersed in CH_2Cl_2 solution. ^c E_{0-0} was determined from intersection of the tangent of absorption on TiO_2 film and the X axis by $1240/\lambda$. ^d The oxidation potentials of the dyes were measured in solution with TBAPF₆ (0.1 M) as electrolyte, ferrocene/ferrocenium (Fc/Fc^+) as an internal reference and converted to NHE by addition of 440 mV. ^e E_{LUMO} were calculated by $E_{\text{HOMO}} - E_{0-0}$.

peak wavelengths on the TiO_2 film are blue-shifted 10 nm, 11 nm and 23 nm for **TJ101**, **TJ102** and **TJ101R**, respectively, with respect to these dyes in CH_2Cl_2 diluted solution. Such phenomenon is attributed to the aggregation of these dyes on TiO_2 surface and deprotonation of carboxylic acid upon adsorption onto the TiO_2 surface. Therefore, the addition of CDCA as co-adsorbent in dye bath is essential for DSSCs to restrain dye aggregation.

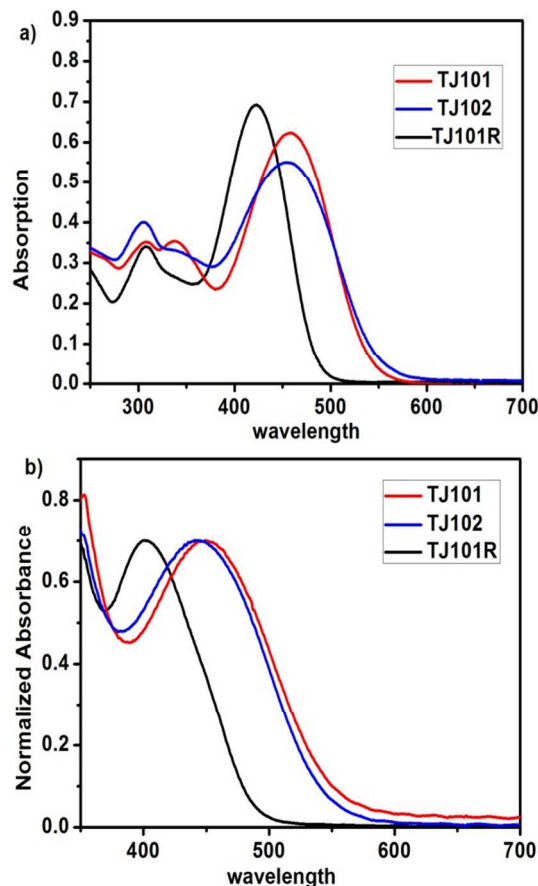


Fig.2 Absorption spectra of **TJ101**, **TJ102** and **TJ101R** in diluted CH_2Cl_2 solution (a); on the TiO_2 (b)

The electrochemical properties of **TJ101**, **TJ102** and **TJ101R** in CH_2Cl_2 have been studied by cyclic voltammetry and the corresponding data are presented in Table 1. The HOMO levels of **TJ101**, **TJ102** and **TJ101R** are more positive than the redox potential of I^-/I_3^- (0.42 vs NHE)²⁸ with 0.61 V, 0.62 V,

0.67 V versus NHE, respectively, demonstrating that the oxidized dyes can be regenerated by the electrolyte effectively. The values of LUMO levels, ranging from -1.62 V to -1.87 V versus NHE, are more negative than the conduction band (CB) of TiO₂ (-0.5 V vs NHE).²⁸ Therefore the electron can be injected into the CB of TiO₂ effectively. Noticeably, the introduction of pyridinium has a beneficial influence on the values of LUMO. The LUMO levels of **TJ101** and **TJ102** have a positive shift in comparison to the LUMO levels of **TJ101R**, which is mainly caused by the enhanced withdrawing ability of electron acceptor. Thus the band energy gap (E_{0-0}) was decreased for **TJ101** (2.23 eV) and **TJ102** (2.30 eV). Additionally, the LUMO values of **TJ101**, with different positions of carboxyl as anchoring group, is more negative than that of **TJ102**, which can be attributed to a better withdrawing synergistic effect of the carboxyl group with pyridinium ring for **TJ101** than that for **TJ102**.

Calculation study

To further investigate the electronic properties of **TJ** series of dyes, density functional theory calculations are employed to analyze these dyes at B3LYP/6-31G*level. The electron

distribution of the HOMO and LUMO of **TJ101-TJ102** and **TJ101R** are shown in Table 3. From the calculation result, it is easy to find that for **TJ101R**, the electron density distribution of HOMO and LUMO overlaps on the π -bridge part. However, for **TJ101** and **TJ102**, the electron density distribution of HOMO is originally located at the donor moiety (TPA), while the electron density of LUMO is located at the acceptor unit. Hence, different from **TJ101R**, **TJ101** and **TJ102** can get obvious electron separation. This is mainly due to the stronger electron withdrawing ability of pyridinium with respect to **TJ101R**.

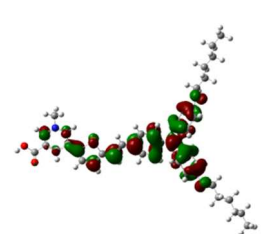
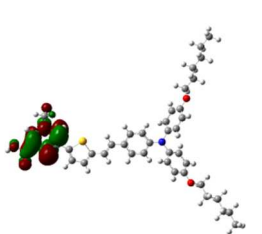
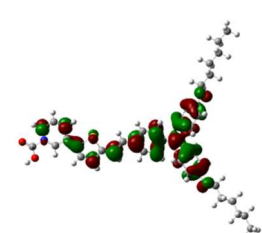
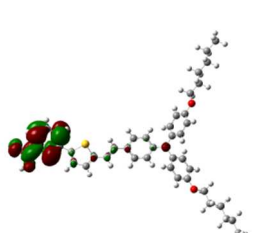
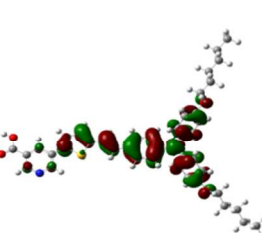
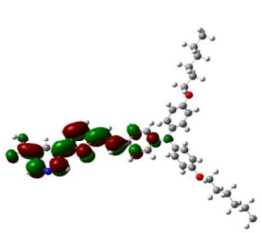
Photovoltaic and Photoelectrochemical Properties

The photocurrent density- photovoltage (J - V) curves of DSSCs based on dyes **TJ101-TJ102** and **TJ101R** are tested under standard AM 1.5G illumination. As is present in Figure 3, in the absent of the CDCA, photon-to-electron conversion efficiency, ranging from 3.2% to 3.9%, have been achieved for the devices based on **TJ101**, **TJ102** and **TJ101R**. Coadsorbent of CDCA is often employed to suppress the dye aggregation by coadsorption with sensitizer on TiO₂ surface, thus improving the photovoltaic performance. Therefore, CDCA is added into the dye bath and expected to achieve a more excellent photovoltaic performance.

Table 2 Photovoltaic performance of DSSCs based on **TJ101**, **TJ102** and **TJ101R**

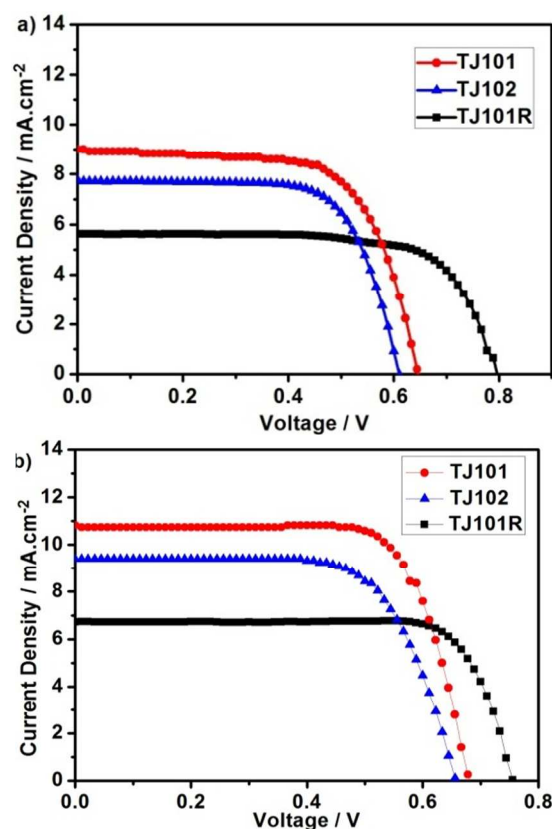
Dye	CDCA	V_{oc} (mV)	J_{sc} (mA cm ⁻²)	FF (%)	η (%)
TJ101	0	646	8.9	66.7	3.9
	saturated	680	10.8	74.2	5.4
TJ102	0	611	7.7	70.4	3.3
	saturated	644	9.4	69.1	4.2
TJ101R	0	796	5.6	71.3	3.2
	saturated	752	6.7	78.5	4.0

Table 3 Electron distribution in HOMO and LUMO levels of **TJ101**, **TJ102** and **TJ101R**

Dye	HOMO	LUMO
TJ101		
TJ102		
TJ101R		

With the addition of CDCA, all the dyes (**TJ101**, **TJ102** and **TJ101R**) have a great improvement on J_{sc} values and the conversion efficiency. Compared with **TJ101R**, with the introduction of pyridinium, a higher short-current density (J_{sc}) is obtained for **TJ101** and **TJ102**, respectively. The explanation for the higher short-current density of pyridinium dyes can be mainly attributed to the broader absorption spectra compared to that for **TJ101R**. Specifically, for **TJ101**, open circuit voltage (V_{oc}) increased from 646 mV to 680 mV, J_{sc} is improved by 1.9 mA cm⁻² and correspondingly η is improved to 5.4%. What's more, the device sensitized by **TJ102** under the same condition shows relatively low J_{sc} and η compared to the device based on **TJ101**. Considering that the main difference between **TJ101** and **TJ102** is the position of carboxyl in the acceptor, when carboxyl group is on the pyridine ring, a better conjugated effect could be achieved for **TJ101** than that for **TJ102**, which is beneficial for excited electron injection.

The incident photon-to-current conversion efficiency (IPCE) spectra of the dyes are displayed in Figure 4. From the test results, it is easy to find that the DSSCs using **TJ101**, **TJ102** and **TJ101R** without CDCA as coadsorbent show lower IPCE values when compared to the DSSCs employed **TJ101**, **TJ102** and **TJ101R**

**Fig.3** a) J - V curves of DSSCs based on **TJ101**, **TJ102** and **TJ101R** without CDCA as coadsorbent; b) J - V curves of DSSCs based on **TJ101**, **TJ102** and **TJ101R** with CDCA as coadsorbent

with CDCA as coadsorbent in the same region, manifesting that the addition of CDCA facilitate the electron injection and charge collection.

With the addition of CDCA, it can be noted that the IPCE spectrum response based on **TJ101R** is ended at 590 nm and the highest IPCE value is close to 90% in the range of 400-500 nm. In contrast, although the IPCE maximum value of **TJ101** and **TJ102** are lower than **TJ101R**, they exhibit broader IPCE spectra response in 350 to 600 nm, which keeps accord with the absorption spectra on TiO₂ film (Figure 1). Moreover, the IPCE spectrum for the device based on **TJ101** is slightly higher than that of **TJ102** in the same region, showing a higher electron injection efficiency and electron collection efficiency of the *m*-carboxyl-*N*-methylpyridinium group.

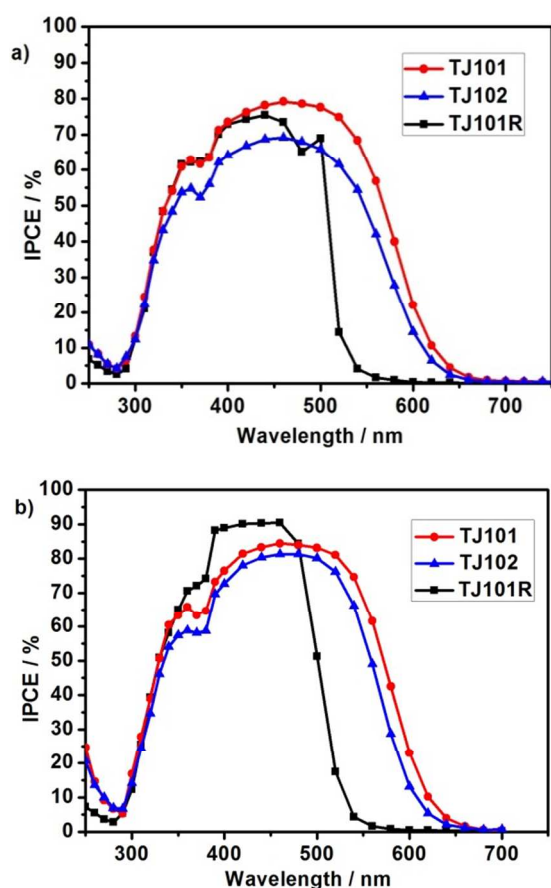


Fig.4 a) IPCE spectra of DSSCs based on **TJ101**, **TJ102** and **TJ101R** without CDCA as coadsorbent; b) IPCE spectra of DSSCs based on **TJ101**, **TJ102** and **TJ101R** with CDCA as coadsorbent

Electrochemical impedance spectroscopy analysis

Electrochemical impedance spectroscopy (EIS) analysis was introduced to study interface charge transfer processes in DSSCs based on **TJ101** and **TJ102**. The impedance spectroscopy was carried out by subjecting the cell to the dark conditions at room temperature and to the bias at -0.8 V which was scanned from 10^6 to 10^{-2} Hz. The alternate current (AC) amplitude was set at 10 mV. The Nyquist plots are displayed in Figure 5. The larger semicircles in lower frequency range (100 Hz to 1 KHz) reflect the recombination resistance (R_{rec}) on the surface of TiO_2 /electrolyte/dye interface, while the smaller semicircle in higher frequency range corresponds to charge transfer resistance (R_{ce}) on the surface of Pt/electrolyte interface.

Any difference can be showed by the two cells based on **TJ101** and **TJ102** in the larger semicircle (R_{rec}) and smaller semicircle (R_{ce}). Noticeably, The R_{rec} for devices based on **TJ101R** is 86 ohm, which is much larger than that of **TJ101** and **TJ102**, indicating that the recombination on the TiO_2 /electrolyte/dye interface can be suppressed effectively for dye **TJ101R**. This phenomenon is reflected on the trend of the V_{oc} . The V_{oc} of devices based on **TJ101R** (795 mV) is much higher than devices based on **TJ101** (646 mV) and **TJ102** (611 mV) in the absent of CDCA. So the introduction of pyridinium as

the acceptor group has a negative effect on the improvement of V_{oc} .

With the addition of CDCA, there is an increase of the R_{rec} for **TJ101** and **TJ102**, respectively. It can be seen from the Nyquist plots (Figure 5b) that the diameters of the larger semicircles in lower frequency is 27.4, 25.1 ohm for **TJ101** and **TJ102**, respectively, which result in the improvement of V_{oc} of **TJ101** (680 mV) and **TJ102** (644 mV). However, the addition of CDCA leads to a decrease of **TJ101R** in the larger semicircle. These results showing that the CDCA can be applied into the pyridinium dyes for improving the V_{oc} . At the same time, for **TJ101** and **TJ102**, the electron recombination can be blocked more effectively for **TJ101** than **TJ102**, as a result of the different position of carboxyl in the pyridine ring. These results suggest that different acceptor groups indeed have large effect on the electron recombination between the TiO_2 film and the electrolyte.

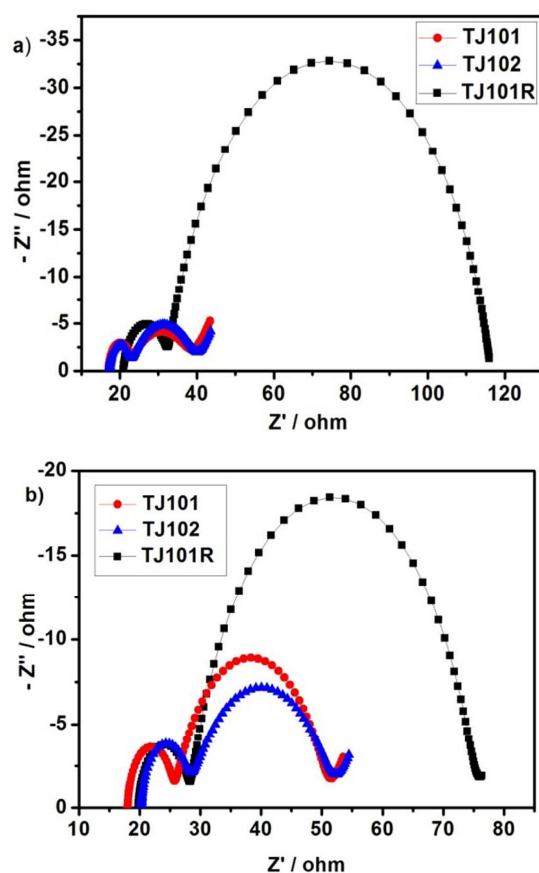


Fig.5 a) Nyquist plots of DSSCs based on dye **TJ101**, **TJ102** and **TJ101R** without CDCA as co-adsorbent; b) Nyquist plots of DSSCs based on dye **TJ101**, **TJ102** and **TJ101R** with CDCA as co-adsorbent

Conclusions

In summary, two metal-free organic dyes with pyridinium (m-carboxyl-*N*-methylpyridinium, *N*-methylcarboxylpyridinium) as the acceptor and anchoring group have been synthesized. The

physical, electrochemical and photovoltaic properties of the dyes **TJ101** and **TJ102** are systematically investigated. It can be found that the introduction of pyridinium as acceptor lead to a red-shifted absorption spectrum and the introduction of pyridinium to synthesize the dyes have favourable effects on improving the overall cell performance, but adverse effects on V_{oc} . With the different positions of the carboxyl in the pyridine ring, a maximal photon-to-electron conversion efficiency of 5.4% ($J_{sc} = 10.8 \text{ mA cm}^{-2}$, $V_{oc} = 680 \text{ mV}$, $FF = 74.2\%$) under AM 1.5 irradiation is obtained for the device based on **TJ101**, while for the devices sensitized by dye **TJ102** achieves the conversion efficiency of 4.2%. Based on these analyses, it can be concluded that the m-carboxyl-*N*-methylpyridine with withdrawing synergistic effect of the carboxyl group and pyridinium ring shows excellent DSSCs performance. Moreover, a great improvement of the overall cell performance based on **TJ101** and **TJ102** is improved by the addition of CDCA. This result will lay a foundation for the further pyridinium molecular design in DSSCs.

Acknowledgements

We gratefully acknowledge the financial support of this work from China Natural Science Foundation (Grant 21276044, 21120102036, 91233201), the National Basic Research Program of China (Grant No. 2014CB239402), the Swedish Energy Agency, K&A Wallenberg Foundation.

Notes and references

^a State Key Laboratory of Fine Chemicals, DUT-KTH Joint Education and Research Centre on Molecular Devices, Dalian University of Technology(DUT), 2 Linggong Rd, 116024 Dalian, China. E-mail: yangxc@dlut.edu.cn; Fax: +86 411 84986250; Tel: +86 411 84986247

^b KTH Royal Institute of Technology, School of Chemical Science and Engineering, Department of Chemistry, Teknikringen 30, 10044 Stockholm, Sweden. E-mail: lichengs@kth.se; Fax: +46 8 791 2333; Tel: +46 8 790 8127

Electronic Supplementary Information (ESI) available: [details of any supplementary information available should be included here]. See DOI: 10.1039/b000000x/

1. B. O'Regan and M. Grätzel, *Nature*, 1991, **353**, 737.

2. S. Mathew, A. Yella, P. Gao, R. Humphry-Baker, B. F. Curchod, N. Ashari-Astani, I. Tavernelli, U. Rothlisberger, M. K. Nazeeruddin and M. Grätzel, *Nature chemistry*, 2014, **6**, 242.

3. D. Kuang, S. Ito, B. Wenger, C. Klein, J.-E. Moser, R. Humphry-Baker, S. M. Zakeeruddin and M. Grätzel, *Journal of the American Chemical Society*, 2006, **128**, 4146.

4. M. K. Nazeeruddin, F. De Angelis, S. Fantacci, A. Selloni, G. Viscardi, P. Liska, S. Ito, B. Takeru and M. Grätzel, *Journal of the American Chemical Society*, 2005, **127**, 16835.

5. M. K. Nazeeruddin, A. Kay, I. Rodicio, R. Humphry-Baker, E. Mueller, P. Liska, N. Vlachopoulos and M. Grätzel, *Journal of the American Chemical Society*, 1993, **115**, 6382.

6. T. Bessho, S. M. Zakeeruddin, C. Y. Yeh, E. W. Diau and M. Grätzel, *Angewandte Chemie*, 2010, **49**, 6646.

7. Y. C. Chang, C. L. Wang, T. Y. Pan, S. H. Hong, C. M. Lan, H. H. Kuo, C. F. Lo, H. Y. Hsu, C. Y. Lin and E. W. Diau, *Chemical communications*, 2011, **47**, 8910.

8. H. He, A. Gurung, L. Si and A. G. Sykes, *Chemical communications*, 2012, **48**, 7619.

9. Y. Liu, N. Xiang, X. Feng, P. Shen, W. Zhou, C. Weng, B. Zhao and S. Tan, *Chemical communications*, 2009, 2499.

10. T. Ripolles-Sanchis, B. C. Guo, H. P. Wu, T. Y. Pan, H. W. Lee, S. R. Raga, F. Fabregat-Santiago, J. Bisquert, C. Y. Yeh and E. W. Diau, *Chemical communications*, 2012, **48**, 4368.

11. J. Warnan, Y. Pellegrin, E. Blart and F. Odobel, *Chemical communications*, 2012, **48**, 675.

12. C.-L. Wang, C.-M. Lan, S.-H. Hong, Y.-F. Wang, T.-Y. Pan, C.-W. Chang, H.-H. Kuo, M.-Y. Kuo, E. W.-G. Diau and C.-Y. Lin, *Energy & Environmental Science*, 2012, **5**, 6933.

13. S.-L. Wu, H.-P. Lu, H.-T. Yu, S.-H. Chuang, C.-L. Chiu, C.-W. Lee, E. W.-G. Diau and C.-Y. Yeh, *Energy & Environmental Science*, 2010, **3**, 949.

14. W. Zhu, Y. Wu, S. Wang, W. Li, X. Li, J. Chen, Z.-s. Wang and H. Tian, *Advanced Functional Materials*, 2011, **21**, 756.

15. Y. Shi, R. B. M. Hill, J.-H. Yum, A. Dualeh, S. Barlow, M. Grätzel, S. R. Marder and M. K. Nazeeruddin, *Angewandte Chemie International Edition*, 2011, **50**, 6619.

16. S. Ito, H. Miura, S. Uchida, M. Takata, K. Sumioka, P. Liska, P. Comte, P. Pechy and M. Grätzel, *Chemical communications*, 2008, 5194.

17. S. Paek, H. Choi, C. Kim, N. Cho, S. So, K. Song, M. K. Nazeeruddin and J. Ko, *Chemical communications*, 2011, **47**, 2874.

18. T. Horiuchi, H. Miura and S. Uchida, *Chemical communications*, 2003, 3036.

19. W. Zeng, Y. Cao, Y. Bai, Y. Wang, Y. Shi, M. Zhang, F. Wang, C. Pan and P. Wang, *Chemistry of Materials*, 2010, **22**, 1915.

20. H. N. Tsao, C. Yi, T. Moehl, J. H. Yum, S. M. Zakeeruddin, M. K. Nazeeruddin and M. Grätzel, *ChemSusChem*, 2011, **4**, 591.

21. J. Yang, P. Ganesan, J. Teuscher, T. Moehl, Y. J. Kim, C. Yi, P. Comte, K. Pei, T. W. Holcombe, M. K. Nazeeruddin, J. Hua, S. M. Zakeeruddin, H. Tian and M. Grätzel, *J Am Chem Soc*, 2014, **136**, 5722.

22. D. P. Hagberg, X. Jiang, E. Gabrielsson, M. Linder, T. Marinado, T. Brinck, A. Hagfeldt and L. Sun, *Journal of Materials Chemistry*, 2009, **19**, 7232.

23. J. Zhao, X. Yang, M. Cheng, S. Li and L. Sun, *ACS applied materials & interfaces*, 2013, **5**, 5227.

-
24. Y. Ooyama, S. Inoue, T. Nagano, K. Kushimoto, J. Ohshita, I. Imae, K. Komaguchi and Y. Harima, *Angewandte Chemie*, 2011, **50**, 7429.
25. J. H. Delcamp, A. Yella, M. K. Nazeeruddin and M. Grätzel, *Chemical communications*, 2012, **48**, 2295.
- 5 26. M. Cheng, X. Yang, C. Chen, J. Zhao, Q. Tan and L. Sun, *Physical chemistry chemical physics : PCCP*, 2013, **15**, 17452.
27. J. Zhao, X. Yang, M. Cheng, S. Li, X. Wang and L. Sun, *Journal of Materials Chemistry A*, 2013, **1**, 2441.
28. K. Hara, T. Sato, R. Katoh, A. Furube, T. Yoshihara, M. Murai, M.
10 Kurashige, S. Ito, A. Shinpo, S. Suga and H. Arakawa, *Advanced Functional Materials*, 2005, **15**, 246.